Redox Biology 19 (2018) 179–189

Contents lists available at ScienceDirect

Redox Biology

journal homepage: www.elsevier.com/locate/redox

Research Paper

DNA hypermethylation-mediated downregulation of antioxidant genes contributes to the early onset of cataracts in highly myopic eyes

Xiangjia Zhu[a,b,c,d,1], Dan Li[a,b,c,d,1], Yu Du[a,b,c,d,1], Wenwen He[a,b,c,d], Yi Lu[a,b,c,d,*]

[a] Department of Ophthalmology, Eye and Ear, Nose, and Throat Hospital of Fudan University, 83 Fenyang Road, Shanghai 200031, China
[b] Key Laboratory of Myopia, Ministry of Health, 83 Fenyang Road, Shanghai 200031, China
[c] Eye Institute of Eye and Ear, Nose, and Throat Hospital of Fudan University, 83 Fenyang Road, Shanghai 200031, China
[d] Key Laboratory of Visual Impairment and Restoration of Shanghai, Fudan University, 83 Fenyang Road, Shanghai 200031, China

ARTICLE INFO

Keywords:
Cataract
High myopia
DNA methylation
Oxidative stress
GSTP1
TXNRD2

ABSTRACT

High myopia is recognized as a risk factor for earlier onset of nuclear cataracts. One possible explanation for this is that lenses in highly myopic eyes are exposed to higher levels of oxygen than normal eyes owing to earlier vitreous liquefaction and, hence, are subjected to oxidative insults. Here, we first compared the methylation levels of six essential antioxidant genes (GSTP1, NRF2, OGG1, TXN, TXNRD1 and TXNRD2) between highly myopic cataract (HMC) and age-related cataract (ARC) lens epithelial samples via Sequenom MassARRAY. We found that specific CpG units in the promoters of GSTP1 and TXNRD2 were hypermethylated and that the expression levels of these two genes were lower in the HMC group than in the ARC group. A luciferase reporter assay confirmed the significance of differentially methylated fragments in the activation of transcription. The importance of GSTP1 and TXNRD2 in antioxidant capacity was confirmed by overexpression or knockdown experiments on cultured lens epithelial cells (LECs). In addition, the expression of DNA methyl transferase 1 (DNMT1) was higher in the lens epithelium of HMC patients than that of ARC patients, and the expression of GSTP1 and TXNRD2 was upregulated by use of a DNMT inhibitor in cultured LECs. Finally, we mimicked the intraocular environment of highly myopic eyes by treating LECs with hydrogen peroxide (H_2O_2) and observed both alterations in the methylation status of the GSTP1 and TXNRD2 promoters and time-dependent altered expression levels. Therefore, we propose that in an environment with high oxygen, in which lenses in highly myopic eyes are immersed, there exists a vicious cycle composed of increased oxidative stress and decreased enzymatic antioxidants via the hypermethylation of antioxidant genes.

1. Introduction

Patients with prescriptions higher than − 6.00 D or an axial length above 26 mm are defined as high myopes and tend to develop rapid, progressive nuclear cataracts with a higher grade than normal people [1–3]. Based on the latest data on vision screening and demographic census, it is estimated that there are currently at least three hundred million patients with high myopia worldwide, especially in East Asia [4–6]. Accordingly, highly myopic cataracts (HMCs) are more frequently observed with the rapidly growing incidence of high myopia.

In normal eyes, the posterior surface of the lens is separated from the inner surface of the retina by an intact vitreous body, which helps preserve the low-oxygen environment surrounding the lens [7]. However, in highly myopic eyes, vitreous gel degeneration occurs much earlier and on a greater scale than in nonmyopic eyes [8], possibly subjecting the lens to higher concentrations of O_2. Elevated oxidative stress may then induce damage to the lens epithelial cells (LECs), the center of normal lens metabolism, and consequently lead to lens opacity.

Our previous study found that the promoter of the CRYAA gene, encoding a major structure protein, αA- crystallin, in the lens, is hypermethylated and hence downregulated in the lens of HMC patients, which could be one of the mechanisms that explains the higher severity

Abbreviations: HMC, highly myopic cataract; ARC, age-related cataract; ARNC, age-related nuclear cataract; LEC, lens epithelial cell; GSTP1, glutathione S-transferase pi 1; TXNRD2, thioredoxin reductase 2; DNMT1, DNA methyl transferase 1; T-AOC, total antioxidant capacity; OE, overexpress; KD, knockdown; ABTS, 2,2′-azino-bis (3-ethylbenzothiazoline-6-sulfonic acid); MDA, malondialdehyde; TBA, thiobarbituric acid; 5-Aza, 5-Aza-2′-deoxycytidine; CCK-8, cell counting kit 8

* Corresponding author.
E-mail address: luyieent@126.com (Y. Lu).
[1] These authors contribute equally to the study.

https://doi.org/10.1016/j.redox.2018.08.012
Received 5 June 2018; Received in revised form 20 August 2018; Accepted 21 August 2018
Available online 23 August 2018

of cataracts in highly myopic eyes [3,9]. In addition to being a structural crystallin, αA- crystallin is also a molecular chaperone with a known function in preventing oxidative damages. These findings prompted us to explore other important antioxidant genes in HMC with the aim of expanding our understanding of this antioxidant system.

To further investigate the underlying epigenetic etiology of HMC, we chose six essential oxidative stress related genes according to previous reports [10–14]: glutathione S- transferase pi 1 (GSTP1), nuclear factor, erythroid like 2 (NRF2), 8-oxoguanine DNA glycosylase (OGG1), thioredoxin (TXN), thioredoxin reductase 1 (TXNRD1) and thioredoxin reductase 2 (TXNRD2). Among these six genes, the expression of GSTP1 has been recently reported to be downregulated in the lens epithelium and cortex of age-related cataracts (ARCs) due to epigenetic alterations, including the hypermethylation of its promoter [15]. Another study showed significantly lower protein and gene expression levels of NRF2 in lenses of increasing age [16]. Furthermore, Nrf2 is a known target for preventing ARC by acting against oxidative stress [17]. OGG1 plays a vital role in DNA repair in response to oxidative stress, the mRNA and protein levels of OGG1 were also significantly reduced in the lens cortex of ARC [18,19]. Furthermore, the CpG islands in the first exon of OGG1 are hypermethylated in the DNA from the lens cortex of ARC [18]. As oxidation defense enzymes functioning in the lens, TXN and TXNRD1 have also been reported to be upregulated under oxidative stress [20].

With a series of preliminary assays including primary screening of CpG methylation levels and the subsequent verification of mRNA levels, we temporarily excluded NRF2, OGG1, TXN and TXNRD1 from the subsequent study and focused on GSTP1 and TXNRD2. In the present study, we aimed to build a relationship between the elevated methylation status of the specific antioxidant genes GSTP1 and TXNRD2 and the decreased antioxidant ability of LECs under oxidative stress, which might be associated with HMC pathogenesis.

2. Materials and methods

2.1. Collection of lens epithelium samples from the patients

Our study was affiliated with the Shanghai High Myopia Study (registered at www.clinicaltrials.gov, NCT 03062085) and was reviewed and approved by the Ethics Committee of the Eye and ENT Hospital of Fudan University, Shanghai, China. Eyes with uveitis, glaucoma, previous trauma, zonular weakness, or diabetic retinopathy were excluded from this study. Lens capsular membranes of 133 ARC patients (axial length ≤ 24.50 mm) and 155 HMC patients (axial length ≥ 26.00 mm) who underwent uneventful cataract surgery at our hospital between January and June 2016 were collected for analysis. These samples were also referred to as lens epithelium in the study. Sterilized balanced salt solution was utilized to rinse off the viscoelastic, blood and iris tissue attached to the membrane. Then samples were kept in phosphate buffered solution (PBS) at 4 °C for immunofluorescent staining within 24 h or immediately frozen and maintained at − 80 °C until further analysis. Written informed consent was obtained from every subject before enrollment. All the procedures adhered to the tenets of the Declaration of Helsinki.

For the sequencing and immunofluorescence staining experiments, lens capsule sample from an individual patient was used as one sample. For the total antioxidant capacity assay (T-AOC), malondialdehyde (MDA) assay, quantitative polymerase chain reaction (qPCR), western blot and enzyme-linked immunosorbent assay (ELISA) assays, two to five pieces of lens capsules were combined as one sample due to the limited amount of proteins or RNA that can be extracted from one piece of lens capsule.

2.2. Measurement of T-AOC and MDA level

The T-AOC was measured by the rapid 3-ethylbenzthiazoline-6-sulfonic acid (ABTS) method (#S0121, Beyotime, China). The peroxidase substrate used in this method is 2,2′-azino-bis ABTS, which produces a soluble end product that is green in color and can be read spectrophotometrically at 405 nm. The presence of antioxidant molecules inhibits production of the colored product, thereby decreasing the absorbance at 405 nm. Trolox was used as a standard antioxidant reagent to generate a standard curve. Lens capsules and cultured LECs were used in this assay. The amount of MDA in lens capsules was detected using an MDA detection kit (#S0121, Beyotime, China) based on the chromogenic reaction of MDA and thiobarbituric acid (TBA). The absorbance of the MDA-TBA adduct was measured at 535 nm. Lens capsule samples were used in the MDA assay. The experiments were conducted according to the manufacturer's instructions.

2.3. Methylation analysis

The Sequenom MassARRAY platform was used to screen the methylation levels of specific loci in the CpG island promoter of the selected genes (GSTP1, NRF2, OGG1, TXN, TXNRD1 and TXNRD2) in the lens epithelium (lens capsule) samples. The CpG island within the promoter of every gene was predicted using an online MethPrimer (http://www.urogene.org/tool.html) [21]. Genomic DNA (gDNA) was extracted from anterior capsule membrane tissues using a DNA extraction kit (#69504, Qiagen, USA). The DNA concentration and purity were measured by NanoDrop 1000 (Thermo Fisher Scientific, USA), with only gDNA of OD A260/280 1.8–2.0 being eligible for further analysis. Qualified gDNA was purified and converted using bisulfite treatment using a DNA methylation kit (#D5001, Zymo Research, USA). Then, DNA regions of interest, which were located in the promoter or near transcription factor binding sites, were amplified. PCR primers were designed using the online software EpiDesigner (www.epidesigner.com, Agena Bioscience, USA), and the primer sequences are listed in Supplementary Table 1. The PCR products were used as a template for transcription and base-specific cleavage reaction using MassCLEAVE kit (#11377, Sequenom, USA). The DNA methylation levels of fragmented samples were detected on a MassARRAY analyzer compact matrix-assisted laser desorption/ ionization time-of-flight mass spectrometry instrument, and EpiTYPER analyzer software (Sequenom) was used to visualize the data. An individual CpG site or a cluster of consecutive CpG sites was defined as a CpG unit in the manufacturer's protocol, where the system always produced one measured value. Lens capsule samples were used in this sequencing method.

To assess the methylation levels of specific sites in GSTP1 and TXNRD2 promoters, the pyrosequencing procedure was performed according to previous studies [22] and the manufacturer's instructions. Lens capsule samples and H_2O_2-treated LECs were used in this sequencing method.

2.4. Assessment of mRNA levels using quantitative PCR

Total RNA from the patients' lens epithelium or cultured cells was extracted using the Trizol reagent (#15596018, Invitrogen, USA) and reverse transcribed into cDNA using the Primescript RT reagent kit (#RR047, Takara, Japan) according to the manufacturer's protocols. mRNA levels of the selected genes were quantified by SYBR Green-based real-time PCR on an ABI 7500 analyzer (Thermo Fisher Scientific). The relative mRNA expression between the target genes and internal control β-actin was calculated using the comparative cycle threshold (CT) method ($2^{-\triangle CT}$). The primer sequences were listed in Supplementary Table 1.

2.5. Assessment of protein levels using western blot assay

Western blot analysis was performed according to standard methods. Briefly, proteins were separated using 10% sodium dodecyl sulfate–polyacrylamide gel electrophoresis, and then transferred to 0.45 μm polyvinylidene difluoride membranes (Merck Millipore,

Germany), which were blocked in 5% nonfat milk for 1 h and incubated with primary antibodies at 4 °C overnight. After washing in a solution of tris-buffered saline and Tween 20, membranes were incubated for 1 h in corresponding secondary antibodies. Detection of the protein was conducted using a chemiluminescence kit (#P90719, Merck Millipore). β-Actin served as the loading control. The primary antibodies included: GSTP1 (#3369, Cell Signaling Technology, USA) and TXNRD2 (#ab181864, Abcam, UK). The dilution of primary antibodies was 1:1000. Secondary antibodies were goat anti-mouse or goat anti-rabbit IgG (H + L) poly-horseradish peroxidase secondary antibody (Jackson Immunoresearch, USA) and the dilution of the secondary antibodies was 1:10,000. Protein extracts from lens capsules of patients, cultured LECs, and whole lenses from experimental mice were used in this assay.

2.6. Detection of GSTP1 and TXNRD2 in lens epithelium using immunofluorescence staining

Lens anterior capsule membranes were attached to the slide with LECs facing upward and fixed in 4% paraformaldehyde for 30 min. Capsules were then permeabilized with PBS containing 0.03% Triton X-100 for 15 min, followed by incubation in PBS solution containing 5% goat serum and 0.1% bovine serum albumin for 1 h to block nonspecific protein binding. Specimens were then incubated with the above-mentioned primary antibodies GSTP1 and TXNRD2 (1:100) at 4 °C overnight. The corresponding secondary antibodies: Alexa Fluor 488-conjugated goat anti-mouse IgG or rhodamine-conjugated goat anti-rabbit IgG (1:450, Jackson Immunoresearch) and Hoechst 33258 (1:2000, Invitrogen) were used to visualize the stained cells. The slides were observed under Leica SP8 confocal microscope (Leica Microsystems, Germany).

ImageJ software (https://imagej.nih.gov/ij/) was used to split the confocal images into single channels. The gray values of the red (TXNRD2) or the green (GSTP1) channels were measured and analyzed.

2.7. Cell culture and transfection

Authentication testing of the human LEC cell line SRA01/04 was performed using short tandem repeat profiling (Shanghai Biowing Applied Biotechnology, China). The SRA01/04 cells were cultured in RPMI-1640 medium (#11875, Gibco, USA) supplemented with 10% fetal bovine serum (#10099141, Gibco) under humidified air containing 5% CO_2 at 37 °C. The medium was changed every other day. To overexpress GSTP1 and TNNRD2 genes in LECs, cDNA sequences were cloned into pcDNA3.1 vector to generate the overexpression constructs. To knock down the expression of GSTP1 and TNNRD2, three short interfering RNAs (siRNAs) of the genes were designed and tested. After qPCR assessment, one siRNA was selected for further cell treatment. LECs were transfected using the transfection reagent (#C10511, RiboBio, China) according to the manufacturer's instructions. In each well of cells in a 12-well culture plate, 1 μg of plasmids or 50 nM siRNA were included in the transfection mixture.

2.8. Measurement of the promoter activity by luciferase reporter assay

To validate the influence of hypermethylated fragments on promoter activity, we separately cloned the GSTP1 and TXNRD2 promoters upstream of the pGL3-luciferase vector. For GSTP1, two constructs of promoter were synthesized: one including the full-length promoter, − 2000/+ 280 region relative to the known transcription start site, and the other including the − 2000/+ 178 region without the fragment including hypermethylated CpG units as previously found by Sequenom MassARRAY. Similarly, two constructs of the TXNRD2 promoter were also synthesized: one including the full-length promoter, − 2000/+ 35 region relative to the known transcription start site and the other including the − 2000/− 25 region without the fragment including hypermethylated CpG units as found by Sequenom MassARRAY. After the verification of sequence syntheses, a luciferase reporter assay was conducted using luciferase assay kit (#E1500, Promega, USA) in accordance with the manufacturer's instructions. Human LEC cell line SRA01/04 were used as host cells in this experiment.

Table 1
Clinical features of ARC and HMC patients during December 2014 and November 2017.

Category	ARC group	HMC group
Number of eyes	8850	4605
Ages (yrs)* **	68.19 ± 7.93	63.26 ± 6.87
Gender (M/F)	2975/5875	1602/3003
Axial length (mm)* **	23.30 ± 0.63	29.84 ± 2.39
LOCS III nuclear color grading* **	2.66 ± 0.60	3.46 ± 1.00
Dark nucleus* **	114 (1.3%)	434 (9.4%)
Vitreous liquefaction* **	5112 (57.8%)	4104 (89.1%)

Values are presented as the mean ± SD (standard deviation). LOCS III: Lens Opacities Classification System III; NC: nuclear color. For ages, axial length and LOCSIII grading, *** $P < 0.001$, Student's *t*-test; for dark nucleus and vitreous liquefaction, ***$P < 0.001$, Chi-square test.

2.9. Detection of DNA-protein binding using electrophoretic mobility shift assay (EMSA)

To investigate the possible transcriptional factor binding to the hypermethylated DNA segments in GSTP1 and TXNRD2 promoters, we conducted EMSA. Nuclear proteins required for EMSA were extracted from LECs on lens capsular membranes using the nuclear extraction reagents, which enable stepwise separation of cytoplasmic and nuclear extracts, according to the given protocol (#78833, Thermo Fisher Scientific). Oligonucleotides of GSTP1 and TXNRD2 segments covering differentially methylated CpG units with and without biotin were all synthesized and purchased from Sangon Biotech (Shanghai, China). The primer sequences are listed in Supplementary Table 1. After pair annealing, the double strand probes were ready for EMSA. EMSA was performed strictly in accordance with the manufacturer's instructions (#20148, Thermo Fisher Scientific).

2.10. DNA methyl transferase (DNMT) inhibitor treatment

Human LECs cell line SRA01/04 were treated with 10 μmol/L 5-Aza-2′-deoxycytidine (5-Aza, Sigma-Aldrich, USA), a DNMT inhibitor, for 3 days. 5-Aza was dissolved in dimethyl sulfoxide (DMSO, Applichem, Germany) and an equivalent amount of DMSO was used as a control treatment. To study the influence of 5-Aza on the expression of GSTP1 and TXNRD2, control and treated cells were collected and used for qPCR and western blot assays.

2.11. Measurement of the protein concentration of DNMT1 using ELISA

Nuclear proteins were isolated from lens capsule samples using the same method as described in Section 2.9. To measure the amount of DNMT1 protein in samples, the EpiQuik™ DNMT1 assay kit (#P-3011, Epigentek Group, USA) was used according to the manufacturer's protocol. Briefly, the samples and the DNMT1 antibody were incubated for 120 min at 37 °C. Subsequently, they were incubated with developing solution for 10 min at room temperature. After the reactions were stopped by addition of the stopping solution, the absorbance was measured at 450 nm using a microplate spectrophotometer (Biotek, USA).

2.12. The influence of hydrogen peroxide (H_2O_2) on the proliferation of LECs

To detect the influence of H_2O_2 treatment on the proliferation of cultured LECs, cell counting kit-8 (CCK-8, #CK04, Dojindo, Japan)

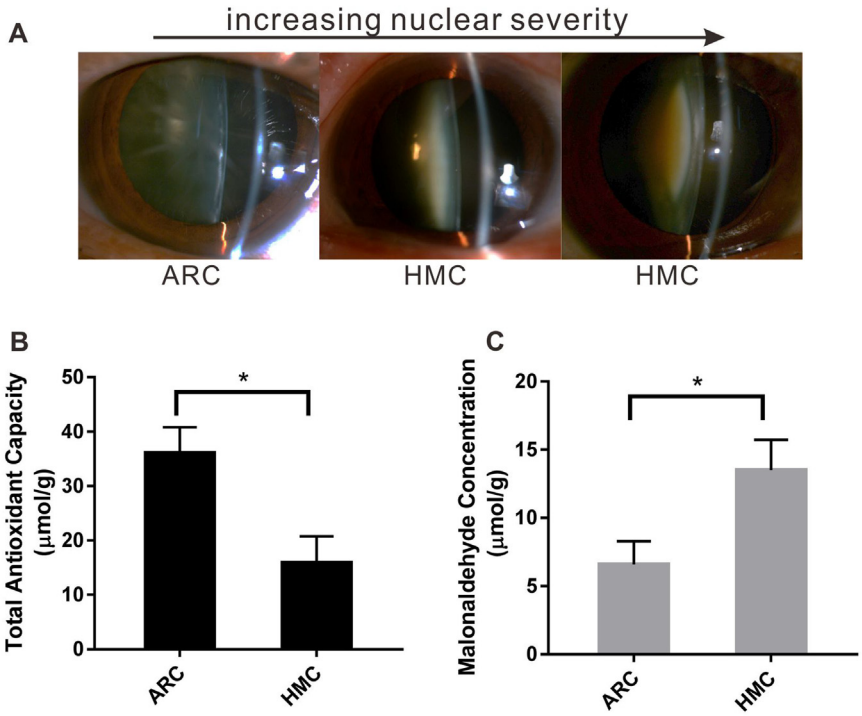

Fig. 1. Higher indexes of oxidative stress in HMC. (A) Representative slit lamp images of lenses with increasing nuclear color of cataract. (**B**) The total antioxidant capacity in the anterior capsular membrane of the HMC group was significantly lower than that of the ARC group. (**C**) The malonaldehyde concentration was significantly higher in HMC. In both assays, n = 3 independent experiments, mean ± SD, unpaired two-tailed Student's *t*-test, *P < 0.05.

assays were conducted. LECs were seeded on culture dish at 4×10^4 cells/mL (denoted as low density), 200 μM H_2O_2 (final concentration) was included in the culture medium. After 24 h, cells images were taken under microscope (DMI 3000B, Leica, Germany), followed by CCK8 assay. The assay was performed in accordance with the manufacturer's instructions.

2.13. The influence of H_2O_2 on the expression and methylation of selected genes

LECs were seeded in culture dishes at a density of 10^5 cells/mL (denoted as high density), and 200 μM H_2O_2 (final concentration) was included in the culture medium. Cells were maintained under H_2O_2 treatment and passaged every 2–3 days. Cells were then harvested from day 0 to day 8 and used for methylation quantification and qPCR. An equivalent amount of H_2O was used as a control treatment.

2.14. Lens-induced myopia mouse model

The animal experiments were approved by the Institutional Animal Care and Use Committee of the Eye and ENT Hospital of Fudan University and were conducted in accordance with the National Institutes of Health guide for the care and use of Laboratory animals (NIH Publications no. 8023, revised 1978). C57BL/6J mice were obtained from Shanghai Slake Laboratory Animal Co., Ltd. To establish a lens-induced high myopia model, 20 wild-type p21 mice were monocularly worn with −25D lenses for four weeks with the contralateral eyes being the controls. Lenses were examined and repositioned every two days and immediately changed when necessary. An infrared photorefractor (Steinbeis Transfer Center, Germany) was used to measure the refraction at the end of the fourth week. Mice with an experimental eye −6.0D more myopic than the self-control eye were considered successful models of lens-induced high myopia and were immediately sacrificed after biometric measurement at the end of the experimental period. Each eye was enucleated and dissected for the lens. Samples were stored at − 80 °C prior to further experimentation.

2.15. Statistical analysis

Data from independent experiments are presented as the mean ± standard deviation (SD). Two-tailed Student's *t*-test was utilized to compare quantitative data between the two groups, and chi-square test was used to compare the sample distribution between two groups (GraphPad Prism version 7.00 for Windows, GraphPad Software, La Jolla California USA, www.graphpad.com). Before the use of Student's *t*-test, Shapiro-Wilk test was used to test for normal distribution. P-values < 0.05 were considered statistically significant: *P < 0.05, **P < 0.01, ***P < 0.001, ****P < 0.0001.

3. Results

3.1. Higher indexes of oxidative stress in highly myopic cataracts

Cataract patients with axial lengths above 26 mm were defined as HMC patients, and those with axial lengths under 24.5 mm were defined as ARC patients. Lens anterior capsular membrane samples were obtained from 155 HMC and 133 nuclear type ARC patients during the continuous curvilinear capsulorhexis step of phacoemulsification conducted by the same surgeon Dr Yi Lu in our hospital. Other than the axial length, no significant differences were found between the two groups of patients in all the listed categories in the Supplementary Table 2. Consequently, the experimental materials from the two groups exhibit relatively uniform baseline features.

On the other hand, to compare the clinical features between ARC and HMC patients, we analyzed the age and grade of nuclear color (which indicates the cataract severity) from 4605 HMC and 8850 nuclear ARC patients admitted to our hospital between December 2014 and November 2017. As presented in Table 1, the average age of the HMC population was significantly younger than that of the ARC population. Additionally, the nuclear color grading of the HMC population was significantly higher than that of ARC. In Fig. 1A, one ARC and two HMC (with increasing nuclear color grading) slit lamp photographs were displayed to represent the cataract severity levels. High myopia was found to be associated with a significantly higher risk of dark nuclear cataract in our previous study [3], and this finding was also

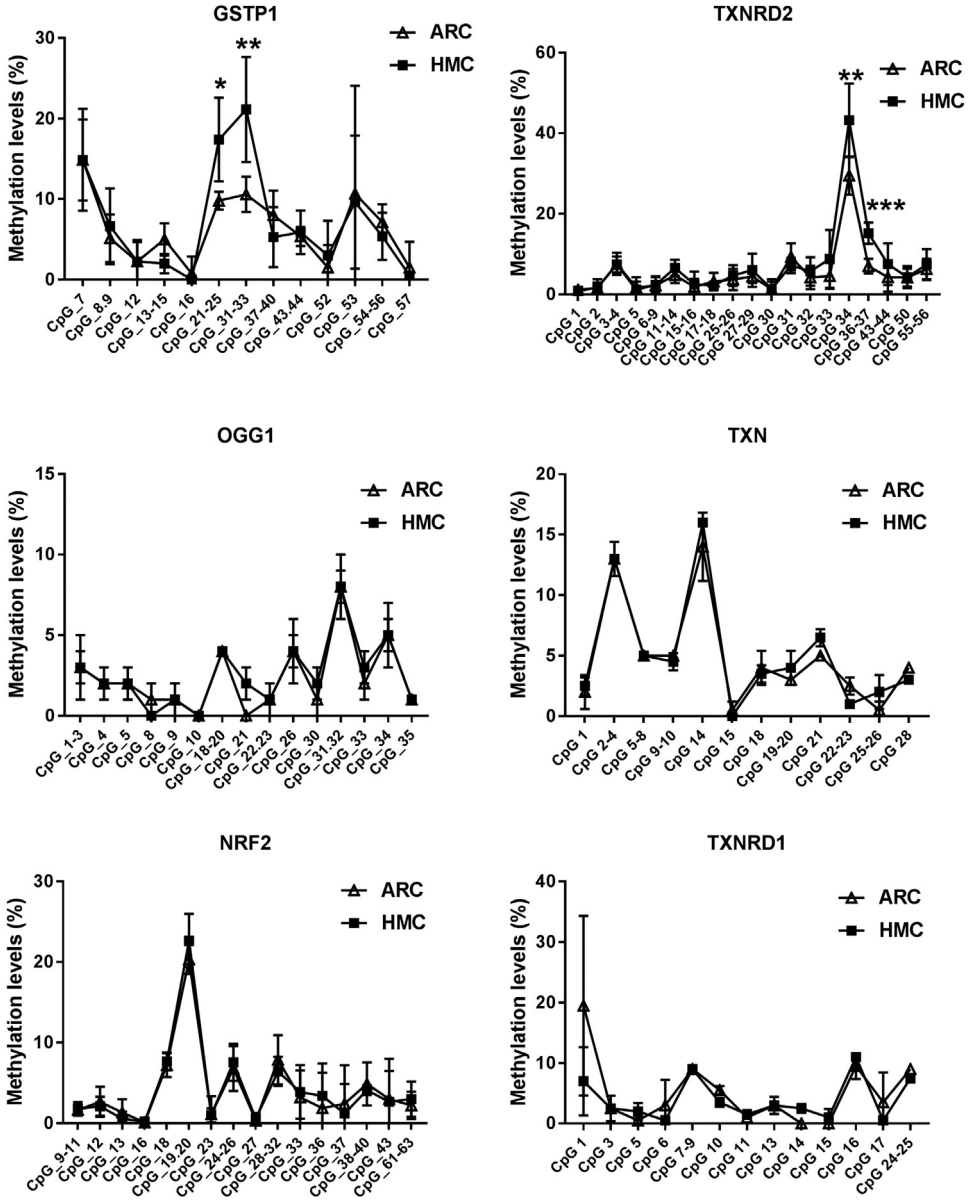

Fig. 2. Methylations status of six antioxidant genes. The methylation levels of GSTP1, TXNRD2, OGG1, TXN, NRF2 and TXNRD1 were measured in ARC and HMC lens epithelium using Sequenom MassARRAY. n = 3 individual patients, mean ± SD, unpaired two-tailed Student's *t*-test, *P < 0.05, **P < 0.01, ***P < 0.001.

verified in Table 1. In addition, 4104 HMC eyes (89.1%) were identified with vitreous liquefaction, and this percentage was significantly higher than that (57.8%) in the ARC group according to the B scan report (Table 1).

To investigate whether there was a difference in antioxidant capacity between HMC and ARC LECs, the anterior capsular membrane of both groups was collected from patients and used for T-AOC assay. Fig. 1B shows that the antioxidant capacity was lower in the HMC group than in the ARC group. In addition, the concentrations of MDA, which is an indicator of lipid peroxidation, were higher in the HMC than that in the ARC group (Fig. 1C), indicating that the lens of highly myopic eyes, with a lower antioxidant capacity, was more susceptible to oxidative injury.

3.2. Promoter hypermethylation and decreased expression of GSTP1 and TXNRD2

To understand why the antioxidant capacity would decrease in HMC lens capsules, we chose to compare the methylation status and expressions of six essential antioxidant genes: GSTP1, TXNRD2, NRF2, OGG1, TXN and TXNRD1 between HMC and ARC lens capsules using Sequenom MassARRAY technology. Validated and reproducible, this method has demonstrated robustness in the quantitative assessment of methylation at multiple CpG sites within large regions of genes and has been confirmed by bisulfite sequencing PCR and pyrosequencing in various studies [23–25]. We quantified the methylation levels of CpG units located within the promoters of these six genes. As shown in Fig. 2, two CpG units in the GSTP1 promoter (#21–25 and #31–33) and two CpG units in the TXNRD2 promoter (#34 and #36–37) showed significantly higher methylation levels in the HMC lens capsule samples than in the ARC samples (see the * symbols in Fig. 2), while little differences in CpG methylation were detected in the other four genes (Fig. 2). Next, we expanded the sample size and confirmed the hypermethylation of one CpG site of GSTP1 (#21–25) and one CpG site of TXNRD2 (#34) (Fig. 3C). In addition, we used pyrosequencing to measure the methylation status of the selected sites: GSTP1 #21–25 and #31–33 (the method failed in the examination of TXNRD2 #34 and 36–37 due to the duplex formation of primer dimers). The result of this

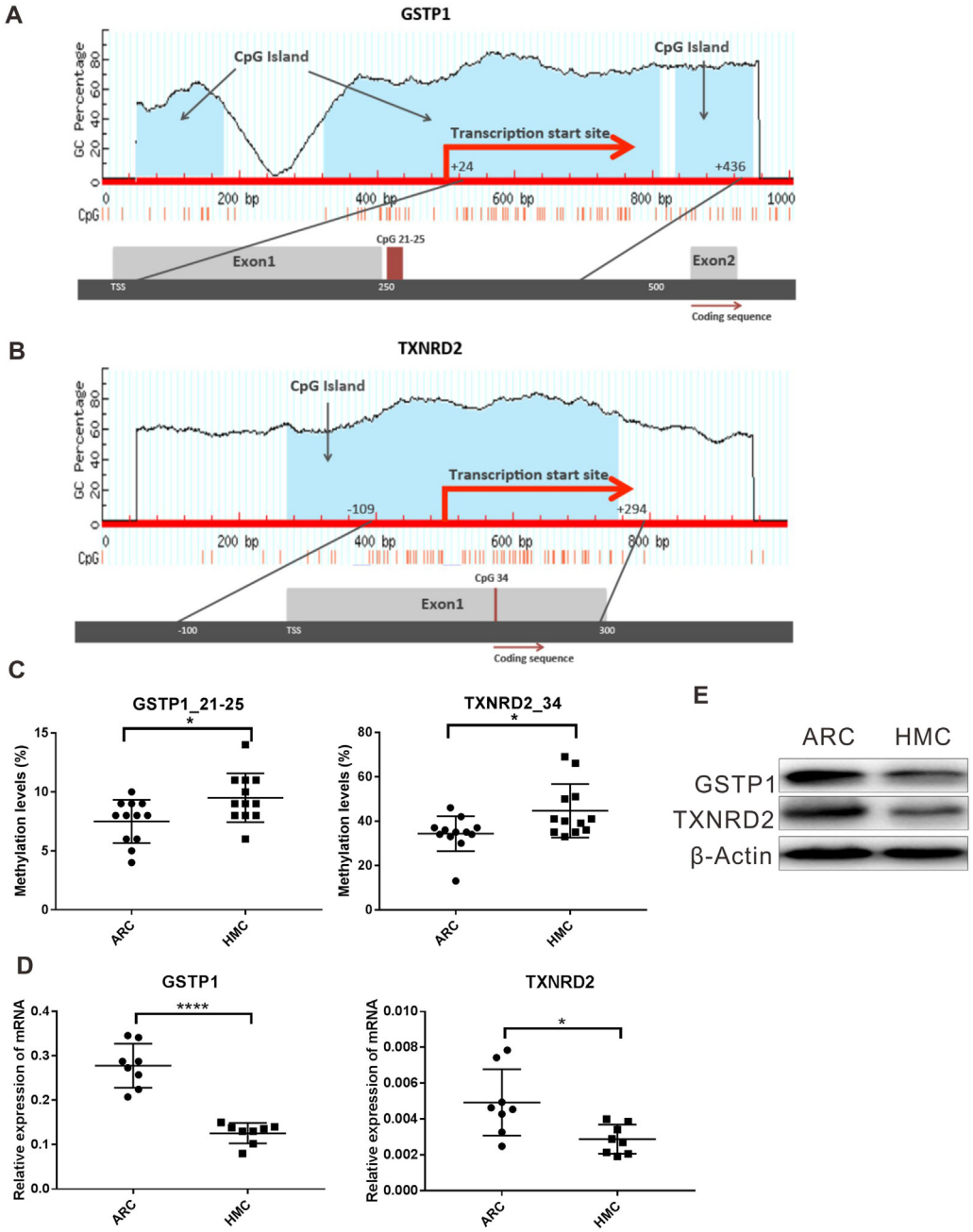

Fig. 3. Hypermethylation in promoter and decreased expression of GSTP1 and TXNRD2 in HMC. (A-B) Diagram of the positions of tested CpG units within the promoters of GSTP1 and TXNRD2. (C) Sequenom MassARRAY experiments using expanded sample size confirmed that one CpG unit in GSTP1 and one in the TXNRD2 CpG island promoter were statistically hypermethylated in the HMC group compared to the ARC group. n = 12 individual patients. (D) Relative mRNA levels of GSTP1, TXNRD2 in ARC and HMC lens epithelium. n = 8 independent experiments. (E) Western blot assay results revealed that the protein levels of both GSTP1 and TXNRD2 were decreased in HMC compared to ARC. mean ± SD, unpaired two-tailed Student's *t*-test, *P < 0.05, ****P < 0.0001.

measurement reconfirmed that the GSTP1 #21–25 CpG unit was hypermethylated in HMC lens capsule samples compared to ARC samples (Supplementary Fig. 1). The specific genomic locations of these differentially methylated sites are marked by arrows in the diagram (Fig. 3A-B). Specifically, in the GSTP1 promoter, the CpG unit 21–25 is located between 8 and 12 bp of the first intron. In the promoter of TXNRD2, CpG unit 34 is located 202 bp downstream of the transcription start site, and 10 bp downstream of the first codon. The mRNA expression levels of GSTP1 and TXNRD2 were measured by qPCR and the protein expression levels of these genes were measured by western blot in both groups of human lens capsules (Fig. 3D-E). In addition, immunofluorescence staining experiments were performed to visualize the protein localization and density in the lens capsular epithelium of 5 subjects from both groups. A semiquantitative analysis of the fluorescence intensity and the representative images are displayed in Fig. 4, showing that the fluorescent signals of GSTP1 and TXNRD2 proteins were lower in the cytoplasm of LECs attached to HMC capsules than those in the ARC group (Fig. 4). More images are provided in Supplementary Figs. 2–5. Overall, the expression levels of GSTP1 and TXNRD2 in the HMC group, compared to the ARC group, were decreased at both the mRNA and protein levels, in agreement with the elevated methylation levels. Meanwhile, the mRNA expression levels of the other four genes, NRF2, OGG1, TXN and TXNRD1 were unchanged between the two groups (Supplementary Fig. 6). Based on these findings, we chose GSTP1 and TXNRD2 for further investigation.

3.3. Altering the expression levels of GSTP1 and TXNRD2 changed the total antioxidant capacity

To investigate whether GSTP1 and TXNRD2 participated in antioxidant defense, we overexpressed (OE) these genes through the use of constructed plasmids or knocked them down (KD) using siRNA of these two genes in cultured LECs and measured the total antioxidant capacity of the transfected cells after 48 h using the T-AOC assay kit. As shown in

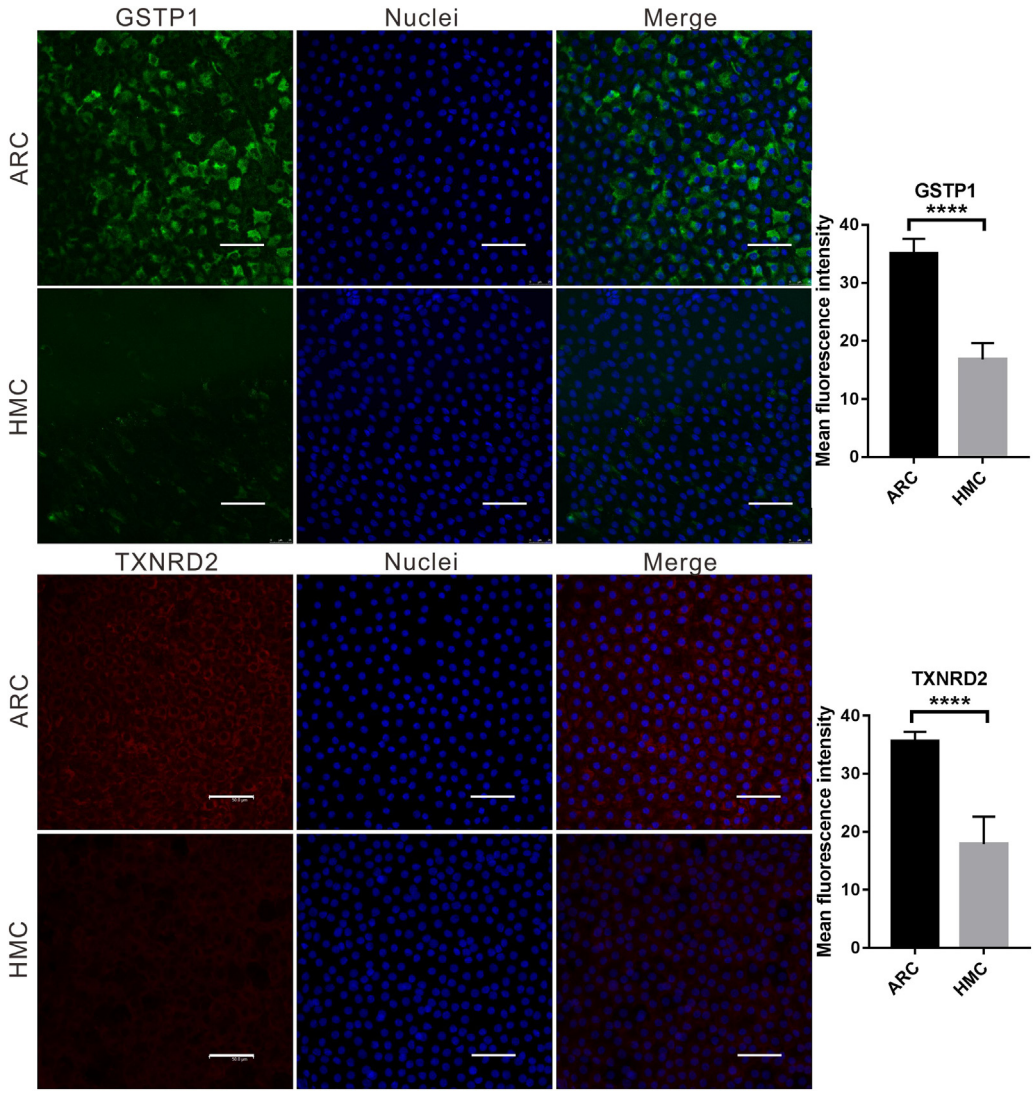

Fig. 4. Immunofluorescence staining of both GSTP1 and TXNRD2 in ARC and HMC lens epithelium. Representative images of GSTP1 (green) or TXNRD2 (red) with nuclei (blue) suggest a reduced expression of these two genes in HMC. scale bar = 50 μm. The results of the quantified fluorescence intensity analysis are presented next to the images. n = 5 individual patients, mean ± SD, unpaired two-tailed Student's *t*-test, ****P < 0.0001.

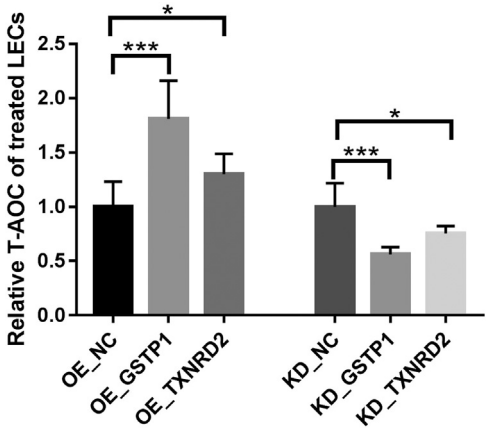

Fig. 5. GSTP1 and TXNRD2 affect T-AOC in cultured LECs. A specific assay kit was used to measure T-AOC in LECs with overexpressed (OE) or knocked down (KD) GSTP1 and TXNRD2. The relative activities were calculated using untreated cells (NC) as control. n = 3 independent experiments, mean ± SD, unpaired two-tailed Student's *t*-test, *P < 0.05, ***P < 0.001.

Fig. 5, the T-AOC increased with GSTP1 OE in LECs, and decreased when it was downregulated. Although a similar trend was observed when the expression of TXNRD2 was manipulated, the effect was less significant, suggesting that TXNRD2 may play a less critical role in antioxidation than GSTP1 when it functions alone. The OE and KD efficiencies were confirmed by qPCR (Supplementary Fig. 7).

3.4. Significance of differentially methylated fragments in the maintenance of promoter activity

As displayed in Fig. 6, luciferase reporter assay showed that the transcriptional activity of both the GSTP1 and TXNRD2 promoters was significantly reduced without differentially methylated segments, suggesting the significance of differentially methylated fragments in the activation of transcription. An EMSA experiment was performed to study the interaction between these differentially methylated segments and transcription factors. The sequences of the DNA probes were selected to cover the CpG units with the largest differences in methylation levels between HMC and ARC. However, no obvious binding of nuclear extracts and DNA probes was detected (Supplementary Fig. 8), suggesting that the methylation of these CpG units was more likely to affect

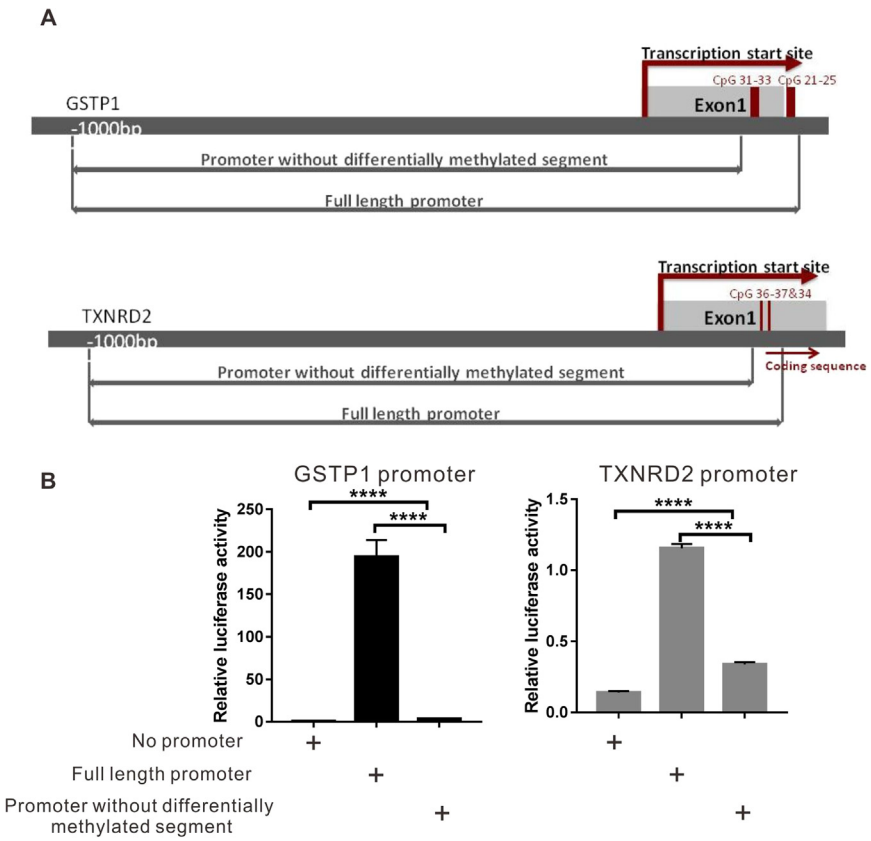

Fig. 6. Significant decrease in promoter activity without hypermethylated fragments in GSTP1/ TXNRD2 genes. (A) Diagrams of the full-length promoter and shortened promoter without hypermethylated fragments of GSTP1 and TXNRD2. (B) Luciferase reporter assay results showed that transcription activity of GSTP1 and TXNRD2 promoter was significantly decreased without DNA fragments, including hypermethylated CpG units found in Sequenom MassARRAY. n = 3 independent experiments, mean ± SD, unpaired two-tailed Student's *t*-test, ****P < 0.0001.

the transcription via an indirect mechanism other than the direct binding with nuclear transcription factors.

3.5. Increased expression of DNMT1 in HMC compared to ARC

To identify the potential upstream regulators of the GSTP1 and TXNRD2 methylation process, we evaluated the expression of three major DNMTs, DNMT1, DNMT3a and DNMT3b, in lens epithelial samples. The qPCR assay results showed that DNMT3a failed to generate an amplification curve, while the CT value of DNMT3b was higher than 33 (the CT value of the endogenous control β-actin was approximately 20), resulting in high variance. In contrast, in the same experiment, the expression of DNMT1 was stable, with a CT value of approximately 30 (Supplementary Table 3). Based on these data, we concluded that DNMT1 is the main methyltransferase existing in the lens epithelium and, therefore, might be the enzyme participating in the hypermethylation of GSTP1 and TXNRD2. As shown in Fig. 7A-B, DNMT1 is more abundant in the HMC group than in the ARC group both at the mRNA level by qPCR and at the protein level as revealed by ELISA, suggesting that DNMT1 catalyzed/maintained the hypermethylation of GSTP1 and TXNRD2 in HMC. In addition, after treatment with 10 μmol/L 5-Aza, a DNMT inhibitor, in LECs culture for 3 days, a significant increase in mRNA and protein levels was observed, which indicated that decreased levels of methylation indeed promoted the expression of these genes (Fig. 7C-D).

3.6. Upregulation of GSTP1 and TXNRD2 methylation by H_2O_2 treatment in a time-dependent manner

To investigate the underlying mechanism of oxidative stress and change in methylation in LECs, we treated cultured LECs with H_2O_2 to mimic the hyperoxic microenvironment in highly myopic eyes. Cell images were taken after we treated the cultured LECs at a low cell density (4×10^4/mL) with 200 μM H_2O_2 for 24 h (Fig. 8A-B). H_2O_2 treatment induced cell death immediately, as the number of living cells and proliferative ability of LECs significantly decreased (Fig. 8C). Then, we treated the LECs with 200 μM H_2O_2 at a high cell density (10^5/mL when plated, cells were passaged every 2–3 days) for 8 days. Under these conditions, cells were able to survive, and we collected cell pellets at different time points for methylation status and mRNA measurements. As shown in Fig. 8D, methylation levels of selected CpG units in the GSTP1 and TXNRD2 promoters (CpG units 21–25 of GSTP1; CpG units 34 of TXNRD2) increased in a time-dependent pattern while the other CpG units in the promoter remained unchanged (data not shown). The locations of the CpG units are shown in Fig. 3A-B. Meanwhile, the expressions of the two genes increased from day 0 to day 6, followed by a steep drop at day 8 (Fig. 8E). In contrast to the findings for GSTP1 and TXNRD2, the expression of DNMT1 remained stable until day 6, when it increased to about 2-fold relative to day 0, indicating that the expressional change in DNMT1 in response to H_2O_2 induction is slower than that of the antioxidant genes GSTP1 and TXNRD2 (Fig. 8E). These results suggest that under H_2O_2 treatment, the expression levels of GSTP1 and TXNRD2 first increased to defend cells from oxidative damage, followed by a decrease possibly resulting from promoter hypermethylation.

4. Discussion

An HMC is a blinding type of cataract frequently observed in Asian countries due to the appallingly high incidence of high myopia in those areas [4,5] and typically features earlier onset and more rapid progression of nuclear cataract [1,2]. The Blue Mountains Eye Study, a large population-based prospective study conducted in Australia, confirmed the association between high myopia and increased incidence of nuclear cataract [26]. In normal eyes, an intact vitreous body is responsible for maintaining a low-oxygen environment surrounding the lens. Previous studies have shown that vitrectomy might lead to nuclear sclerotic cataracts due to alterations in lens metabolism [27,28]. Beebe

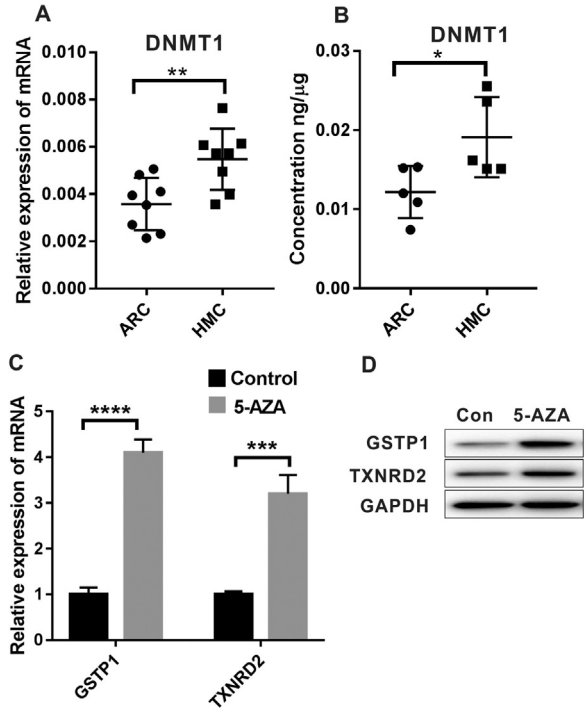

Fig. 7. Higher expression of DNMT1 in the lens epithelium of HMC and increased expression of GSTP1 and TXNRD2 in LECs after treatment with 5-Aza. (**A**) qPCR results showed that the mRNA level of DNMT1 was higher in HMC lens epithelium than in the ARC group. n = 8 independent experiments. (**B**) ELISA results showed that protein level of DNMT1 was higher in HMC lens epithelium than in ARC samples. n = 5 independent experiments. (**C**) qPCR results showed that mRNA levels of both GSTP1 and TXNRD2 in cultured LECs increased significantly after treatment with 5-Aza. n = 3 independent experiments. (**D**) Western blot assay results showed that protein levels of both GSTP1 and TXNRD2 increased in cultured LECs after treatment with 5-Aza. mean ± SD, unpaired two-tailed Student's *t*-test, *P < 0.05, **P < 0.01, ***P < 0.001, ****P < 0.0001.

et al. found that these problems may have resulted from the increased exposure of the lens to the oxygen from the fundus due to the destruction of vitreous gel [7]. Yan et al. removed the vitreous gel of rabbits with vitrectomy and exposed the lens to increased oxygen and found aggravated lens oxidation [29]. The lens may also lose transparency in other conditions related to vitreous destruction, such as high myopia [30,31]. In highly myopic eyes, with much longer axial lengths and larger eyeballs, vitreous liquefaction occurs much earlier than in normal eyes [32], generating a high-oxygen environment surrounding the lens, thus resulting in earlier onset and higher severity of cataracts than those of ARC. Therefore, the antioxidant capacity within the lens plays an essential role in preventing the development of cataracts. In this study, we measured two classic markers related to oxidative stress, T-AOC and MDA, and found significantly lower T-AOC and higher levels of MDA in the HMC group, suggesting that the antioxidant defense of HMC is much weaker than that of ARC. Thus, we propose that the earlier onset of nuclear cataracts in highly myopic eyes is probably related to the higher oxidative stress and the lower antioxidant capacity in HMC than in ARC.

DNA methylation is a classic epigenetic mechanism of gene silencing that participates in various ocular diseases, such as pterygium [33], age-related macular degeneration and retinitis pigmentosa [34]. A high-oxygen environment may induce epigenetic alterations, especially to genes of antioxidant enzymes. In our previous study, we identified that hypermethylation of the CRYAA promoter played an important role in the development of high myopia-induced dark nuclear cataracts [3]. In the present study, we examined the methylation status of six important antioxidant genes as described in the results (Fig. 2), and GSTP1 and TXNRD2 were selected for further study because their promoters were hypermethylated.

GSTP1 is widely expressed in the epithelial tissue of the eyes and belongs to a large supergene family with a powerful capacity in detoxification of xenobiotics and in antioxidant defense, especially during exposure to increased oxygen [35,36]. Glutathione S-transferase (GST) distribution and activity were significantly decreased in cataractous human lens compared with healthy lens [37]. Fan et al. previously reported hypermethylation of the GSTP1 promoter in response to systemic oxidative stress in peripheral mononuclear cells of patients with chronic hepatitis B [38]. Interestingly, Chen et al. reported epigenetic alterations of GSTP1 in age-related nuclear cataracts (ARNCs) and suggested that the methylation levels of two regions of the GSTP1 promoter (− 819 bp to − 533 bp and from − 201 bp to + 86 bp) might be correlated with the severity of ARNCs [15]. In our study, we showed that the methylation level of the GSTP1 promoter was even higher in HMC than in ARC (we can also use ARNCs here, considering that the included ARC samples were all of the nuclear type). Thioredoxin reductase could also catalyze the reduction of numerous oxidized cell constituents, including protein-thiol mixed disulfide. It is crucial to restore thioredoxin, a core antioxidant molecule in the lens, to its reduced state for defense against oxidants. Downregulated TXNRD2, the mitochondrial form of thioredoxin reductase, may weaken the mitochondrial thioredoxin system, resulting in mitochondrial injury to LECs. Our preliminary data showed that in the lens-induced myopia mouse model, the expression of TXNRD2 was also significantly reduced in the lens of the myopic eye, while the GSTP1 level was relatively stable (Supplementary Fig. 9). In addition, the importance of hypermethylated CpG units of GSTP1 and TXNRD2 in transcriptional activity was validated by luciferase reporter assay, as displayed in Fig. 6. However, to confirm the repressive effect of the hypermethylated spots on transcriptional activity, specific methylation of the CpG units 21–25 of GSTP1 and CpG unit 34 of TXNRD2 followed by expression assessment is ideal. Although it is possible to perform such site-specific epigenetic modification using a recently developed DNA editing tool [39], this procedure is beyond our current technical capacity.

Furthermore, the higher expression levels of DNMT1 seemed to be responsible for the elevated levels of methylation in the GSTP1 and TXNRD2 promoters in HMC. In the DNA methyltransferase family, the functions of DNMT1 and DNMT3, including 3a and 3b, were the most ubiquitously expressed in cells. DNMT1 encodes the enzyme that is the most abundant DNA methyltransferase in mammalian cells and is considered the key maintenance methyltransferase, while DNMT3 mostly functions in de novo methylation. Aberrant methylation patterns induced by DNMT1 have been discovered in the initiation of many diseases, such as tumor or developmental abnormalities. Previously, there have also been studies proving the role of DNMT1 in addressing the possible influence of elevated oxidative stress on genome-wide DNA methylation levels [40]. Wu et al. reported that reactive oxygen species might induce site-specific hypermethylation via either the overexpression of DNMTs or the formation of a new DNMT-containing complex that better catalyzes this modification [41]. Our study discovered that, compared to LECs from ARC cases, LECs from HMC cases showed higher expression of DNMT1 at both the mRNA and protein levels, where the LECs were in a condition with higher levels of oxidative stress. Similar to our findings, DNMT1 was found to be upregulated in oxidative stress-related conditions, such as in an Alzheimer disease model in mice [42].

In our hypothesis, the elevated level of oxidative stress would damage the LECs in highly myopic eyes; thus, by treating LECs with H_2O_2, we aimed to simulate the microenvironment of HMC in terms of

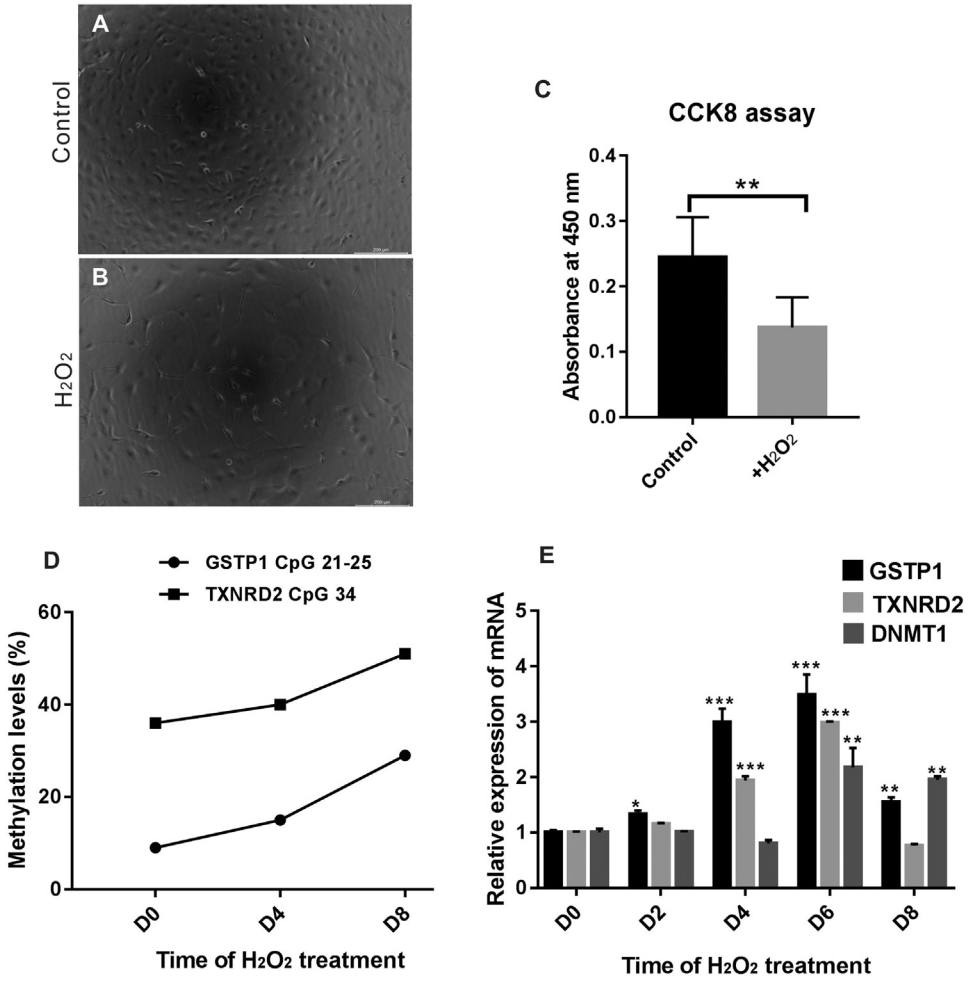

Fig. 8. Upregulation of methylation by H_2O_2 treatment in a time-dependent manner. (**A**) Cell image before H_2O_2 treatment. (**B**) Cell image after 24 h of treatment with 200 μM H_2O_2. (**C**) CCK-8 assay revealed that the proliferation of LECs was significantly decreased after 24 h of treatment with 200 μM H_2O_2. n = 4 independent experiments. (**D**) The methylation levels of selected CpG units in the GSTP1 and TXNRD2 promoters (CpG units 21–25 of GSTP1; CpG units 34 of TXNRD2) increased in a time-dependent pattern under H_2O_2 treatment. (**E**) Under H_2O_2 treatment, the relative mRNA levels of GSTP1 and TXNRD2 gradually increased in the first six days and declined at day 8. The expression of DNMT1 remained stable until day 6, when it increased to about 2-fold relative to day 0. n = 3 independent experiments, mean ± SD, unpaired two-tailed Student's *t*-test, *P < 0.05, **P < 0.01, ***P < 0.001 (each sample was compared to day 0 when statistically analyzed).

oxidative stress. We analyzed the regulation of methylation and gene expression of GSTP1 and TXNRD2 in response to H_2O_2 treatment. Our results indicated that H_2O_2 induction resulted in complex effects. In the present experiment, during a period of 8 days of H_2O_2 treatment, we observed increased expression of these two genes in the middle stage (from day 2 to day 6), followed by a sharp decrease at the late stage (day 6 to day 8) of the treatment period (Fig. 8E). One explanation of this finding would be that under oxidative stress, the expression of these two antioxidant genes would first increase to defend against the high-oxygen environment; on the other hand, the oxidative stress would chronically increase the methylation levels of the gene promoters possibly through upregulation of DNMT1, resulting in a decrease in transcription products of GSTP1 and TXNRD2. This implies that in highly myopic eyes, higher concentrations of oxygen due to earlier vitreous liquefaction are more likely to have a chronic effect, as they might not only cause direct oxidative damage to the lens but also simultaneously lead to impairment of antioxidant capacity through epigenetic regulation.

In summary, we propose a model as depicted in the graphical abstract. In highly myopic eyes, extreme elongation of the eyeball induces early liquefaction of the vitreous body, which elevates the oxygen concentration around the lens. Higher levels of oxidative stress elicit overexpression of DNMT1 and induce hypermethylation of antioxidant genes such as GSTP1 and TXNRD2. Epigenetic modifications then repress the expression of these genes and impair the antioxidant capacity. Combined with our previous studies, we conclude that oxidative stress and DNA methylation might reciprocally influence each other and form a vicious cycle, resulting in earlier onset and greater severity of cataracts in highly myopic eyes.

Acknowledgements

The authors sincerely appreciate the patients for participation. This research was funded by research grants from the National Natural Science Foundation of China (Grant nos. 81470613, 81870642, 81100653, 81670835, and 81270989), Shanghai High Myopia Study Group, International Science and Technology Cooperation Foundation of Shanghai (Grant no. 14430721100), Shanghai Talent Development Fund (Grant no. 201604), Shanghai Youth Doctor Support Program (Grant no. 2014118), and Outstanding Youth Medical Talents Program of Shanghai Health and Family Planning Commission (Grant no. 2017YQ011).

Author contributions

X.J.Z. designed the study; D.L. and Y.D. performed the study; Y.D., D.L. and W.W.H. collected data; Y.D. and D.L. analyzed and interpreted the data; X.J.Z., D.L., and Y.L. wrote, reviewed, and approved the manuscript. All authors have read and approved the manuscript.

Competing interests

None of the authors has any proprietary/financial interest to disclose.

Appendix A. Supporting information

Supplementary data associated with this article can be found in the online version at doi:10.1016/j.redox.2018.08.012

References

[1] E. Kubo, et al., Axial length, myopia, and the severity of lens opacity at the time of cataract surgery, Arch. Ophthalmol. 124 (11) (2006) 1586–1590.
[2] C.W. Pan, et al., Myopia, axial length, and age-related cataract: the Singapore Malay eye study, Investig. Ophthalmol. Vis. Sci. 54 (7) (2013) 4498–4502.
[3] X.J. Zhu, et al., Epigenetic regulation of alphaA-crystallin in high myopia-induced dark nuclear cataract, PLoS One 8 (12) (2013) e81900.
[4] J. Sun, et al., High prevalence of myopia and high myopia in 5060 Chinese university students in Shanghai, Investig. Ophthalmol. Vis. Sci. 53 (12) (2012) 7504–7509.
[5] L.J. Wu, et al., Prevalence and associated factors of myopia in high-school students in Beijing, PLoS One 10 (3) (2015) e0120764.
[6] B.A. Holden, et al., Global prevalence of myopia and high myopia and temporal trends from 2000 through 2050, Ophthalmology 123 (5) (2016).
[7] D.C. Beebe, et al., Vitreoretinal influences on lens function and cataract, Philos. Trans. R. Soc. Lond. B Biol. Sci. 366 (1568) (2011) 1293–1300.
[8] H. Morita, M. Funata, T. Tokoro, A clinical study of the development of posterior vitreous detachment in high myopia, Retina 15 (2) (1995) 117–124.
[9] P. Zhou, et al., Down-regulation and CpG island hypermethylation of CRYAA in age-related nuclear cataract, FASEB J. 26 (12) (2012) 4897–4902.
[10] H. Yan, et al., Thioredoxin, thioredoxin reductase, and alpha-crystallin revive inactivated glyceraldehyde 3-phosphate dehydrogenase in human aged and cataract lens extracts, Mol. Vis. 12 (2006) 1153–1159.
[11] K.Y. Xing, M.F. Lou, Effect of age on the thioltransferase (glutaredoxin) and thioredoxin systems in the human lens, Investig. Ophthalmol. Vis. Sci. 51 (12) (2010) 6598–6604.
[12] R. Elanchezhian, et al., Age-related cataracts: homocysteine coupled endoplasmic reticulum stress and suppression of Nrf2-dependent antioxidant protection, Chem. Biol. Interact. 200 (1) (2012) 1–10.
[13] R. Qi, Z. Gu, L. Zhou, The effect of GSTT1, GSTM1 and GSTP1 gene polymorphisms on the susceptibility of age-related cataract in Chinese Han population, Int. J. Clin. Exp. Med. 8 (10) (2015) 19448–19453.
[14] F. Wang, et al., DL-3-n-butylphthalide delays the onset and progression of diabetic cataract by inhibiting oxidative stress in rat diabetic model, Sci. Rep. 6 (2016) 19396.
[15] J. Chen, et al., Aberrant epigenetic alterations of glutathione-S-transferase P1 in age-related nuclear cataract, Curr. Eye Res. 42 (3) (2017) 402–410.
[16] Y. Gao, Y. Yan, T. Huang, Human age related cataracts: epigenetic suppression of the nuclear factor erythroid 2 related factor 2 mediated antioxidant system, Mol. Med. Rep. 11 (2) (2015) 1442–1447.
[17] X.F. Liu, et al., Nrf2 as a target for prevention of age-related and diabetic cataracts by against oxidative stress, Aging Cell 16 (5) (2017) 934–942.
[18] Y. Wang, et al., Altered DNA methylation and expression profiles of 8-oxoguanine DNA glycosylase 1 in lens tissue from age-related cataract patients, Curr. Eye Res. 40 (8) (2015) 815–821.
[19] Y. Zhang, et al., Expression changes in DNA repair enzymes and mitochondrial DNA damage in aging rat lens, Mol. Vis. 16 (2010) 1754–1763.
[20] H. Liu, et al., Sulforaphane can protect lens cells against oxidative stress: implications for cataract prevention, Investig. Ophthalmol. Vis. Sci. 54 (8) (2013) 5236–5248.
[21] L.C. Li, R. Dahiya, MethPrimer: designing primers for methylation PCRs, Bioinformatics 18 (11) (2002) 1427–1431.
[22] X.J. Zhu, et al., alphaA-crystallin gene CpG islands hypermethylation in nuclear cataract after pars plana vitrectomy, Graefes Arch. Clin. Exp. Ophthalmol. 253 (7) (2015) 1043–1051.
[23] P. Garagnani, et al., Methylation of ELOVL2 gene as a new epigenetic marker of age, Aging Cell 11 (6) (2012) 1132–1134.
[24] G.G. Slaats, et al., DNA methylation levels within the CD14 promoter region are lower in placentas of mothers living on a farm, Allergy 67 (7) (2012) 895–903.
[25] H.E. Suchiman, et al., Design, measurement and processing of region-specific DNA methylation assays: the mass spectrometry-based method EpiTYPER, Front. Genet. 6 (2015) 287.
[26] G.L. Kanthan, et al., Myopia and the long-term incidence of cataract and cataract surgery: the blue mountains eye study, Clin. Exp. Ophthalmol. 42 (4) (2014) 347–353.
[27] S. de Bustros, et al., Nuclear sclerosis after vitrectomy for idiopathic epiretinal membranes, Am. J. Ophthalmol. 105 (2) (1988) 160–164.
[28] G.M. Cherfan, et al., Nuclear sclerotic cataract after vitrectomy for idiopathic epiretinal membranes causing macular pucker, Am. J. Ophthalmol. 111 (4) (1991) 434–438.
[29] H. Yan, et al., Comparison of lens oxidative damage induced by vitrectomy and/or hyperoxia in rabbits, Int. J. Ophthalmol. 10 (1) (2017) 6–14.
[30] F. Simonelli, et al., Lipid peroxidation and human cataractogenesis in diabetes and severe myopia, Exp. Eye Res. 49 (2) (1989) 181–187.
[31] R. Milston, M.C. Madigan, J. Sebag, Vitreous floaters: etiology, diagnostics, and management, Surv. Ophthalmol. 61 (2) (2016) 211–227.
[32] N.M. Holekamp, et al., Myopia and axial length contribute to vitreous liquefaction and nuclear cataract, Arch. Ophthalmol. 126 (5) (2008) 744 (author reply 744).
[33] A.K. Riau, et al., Aberrant DNA methylation of matrix remodeling and cell adhesion related genes in pterygium, PLoS One 6 (2) (2011) e14687.
[34] P. Farinelli, et al., DNA methylation and differential gene regulation in photoreceptor cell death, Cell Death Dis. 5 (12) (2014) e1558.
[35] H. Ahmad, et al., Differential expression of alpha, mu and pi classes of isozymes of glutathione S-transferase in bovine lens, cornea, and retina, Arch. Biochem. Biophys. 266 (2) (1988) 416–426.
[36] T. Nishinaka, et al., Difference in glutathione S-transferase response to oxidative stress between porcine and bovine lens, Exp. Eye Res. 56 (3) (1993) 299–303.
[37] Q.L. Huang, et al., Distribution and activity of glutathione-S-transferase in normal human lenses and in cataractous human epithelia, Curr. Eye Res. 12 (5) (1993) 433–437.
[38] X.P. Fan, et al., Methylation of the Glutathione-S-Transferase P1 gene promoter is associated with oxidative stress in patients with chronic hepatitis B, Tohoku J. Exp. Med. 238 (1) (2016) 57–64.
[39] X.S. Liu, et al., Rescue of fragile X syndrome neurons by DNA methylation editing of the FMR1 gene, Cell 172 (5) (2018) 979–992 (e6).
[40] Y. Niu, et al., Oxidative stress alters global histone modification and DNA methylation, Free Radic. Biol. Med. 82 (2015) 22–28.
[41] Q. Wu, X. Ni, ROS-mediated DNA methylation pattern alterations in carcinogenesis, Curr. Drug Targets 16 (1) (2015) 13–19.
[42] C. Grinan-Ferre, et al., Epigenetic mechanisms underlying cognitive impairment and Alzheimer disease hallmarks in 5XFAD mice, Aging 8 (4) (2016) 664–684.